Nonlinear electrophoresis of non-spherical particles in a rectangular microchannel

Joseph Bentor and Xiangchun Xuan

Department of Mechanical Engineering, Clemson University, Clemson, SC 29634-0921, USA

Correspondence: Prof. Xiangchun Xuan, Department of Mechanical Engineering, Clemson University, Clemson, SC 29634-0921, USA. **E-mail:** xcxuan@clemson.edu.

Abstract

Nonlinear electrophoresis offers advantageous prospects in microfluidic manipulation of particles over linear electrophoresis. Existing theories established for this phenomenon are entirely based on spherical particle models, some of which have been experimentally verified. However, there is no knowledge on if and how the particle shape may affect the nonlinear electrophoretic behavior. This work presents an experimental study of the nonlinear electrophoretic velocities of rigid peanut- and pear-shaped particles in a rectangular microchannel, which are compared with rigid spherical particles of similar diameter and surface charge in terms of the particle slenderness. We observe a decrease in the nonlinear electrophoretic mobility while an increase in the nonlinear index of electric field when the particle slenderness increases from the peanut- to pear-shaped and spherical particles. The values of the nonlinear index for the non-spherical particles are, however, still within the theoretically predicted range for spherical particles. We also observe an enhanced nonlinear electrophoretic behavior in a lower-concentration buffer solution regardless of the particle shape.

Keywords

Electrokinetic / Surface conduction / Nonlinearity / Particle shape / Microfluidics

1 Introduction

In classical electrokinetics, the electrophoretic velocity of particles is proportional to the imposed electric field [1,2]. This linear relationship breaks down under high electric fields (i.e., $\beta = Ea/\phi \gg 1$ with E being the electric field strength, a the particle radius, and ϕ the thermal voltage) and/or for highly charged particles (i.e., $\sigma a/\varepsilon\phi \gg 1$ with σ being the particle's surface charge density and ε the fluid permittivity), where ionic fluxes are induced across the electric double layer (EDL, characterized by the Debye length, $1/\kappa$) because of the surface conduction effect [3-6]. The consequence is the onset of nonlinear electrophoresis whose velocity is predicted based upon a spherical particle model to exhibit a 3- to 3/2-order dependence on the electric field strength [7-10]. This phenomenon has been experimentally investigated with spherical dielectric particles by several research groups [11-15]. It has also been utilized to enhance the trapping and separation of spherical particles [16-20]. A brief overview of these earlier studies was provided in our previous work in early 2023 [21] and is therefore skipped here. Readers interested in this topic are also suggested to refer to the review paper from Khair [22] for a more complete discussion of those theoretical and experimental works published before 2022. We present below a summary of only those papers published since our previous work [21].

Lapizco-Encinas and colleagues published four papers pertaining to nonlinear electrophoresis during this time period. Two of these papers are dedicated to the fundamental understanding of the significant factors in nonlinear electrophoresis. Ernst et al. [23] studied the particle size and charge dependencies of nonlinear electrophoretic velocity for a total of nine distinct types of spherical polystyrene particles. They assessed the experimental data under both the 3- and 3/2-order electric field scaling and obtained the corresponding nonlinear electrophoretic mobilities for each type of particles. They reported that the mobilities in both regimes increase with increasing particle size and decrease with increasing particle charge. Later, Lomeli-Martin et al. [24] divided the commercially available spherical polystyrene particles into three categories based on the difference in their nonlinear electrophoretic behaviors: “type 1” particles travel along with the electroosmotic fluid flow but reverse once the imposed electric field goes beyond a threshold; “type 2” particles travel against the fluid flow and have very small values of nonlinear electrophoretic mobility; “type 3” particles travel along with the fluid flow exhibiting a linear electrophoretic velocity even at extremely high electric fields (~6 kV/cm). The authors concluded from the common features among these particles that size, surface functionalization, and electrical charge can all be determining factors in electrophoresis.

The other two papers from Lapizco-Encinas and colleagues are focused upon the application of nonlinear electrophoresis in size- or charge-based separation of particles and cells. Vaghef-Koodehi et al. [25] presented a continuous separation of particles and cells of similar characteristics through the combined linear and nonlinear DC electrokinetic phenomena in an insulator-based electrokinetic system. The authors developed a spherical particle model in COMSOL to predict the retention times of particles and cells in four distinct separations of binary mixtures at increasing difficulty, from spherical polystyrene particles of different sizes to E. coli vs. S. cerevisiae, B. cereus vs. S. cerevisiae, and B. cereus vs. B. subtilis. Their predictions were reported to agree with the experimentally measured particle/cell retention times with acceptable deviations and variations. In a later work, Ahamed et al. [26] demonstrated the use of DC-biased low-frequency AC voltage to achieve in a similar insulator-based electrokinetic system the separation of same-sized spherical polystyrene particles with ~14 mV zeta potential difference. They again used the spherical particle model in COMSOL, which considers both linear and nonlinear electrophoresis, to examine the effect of fine-tuning AC voltage frequency, amplitude and DC bias, respectively. The numerically optimized value for each of these parameters was used in the experiment, which was found to improve the separation resolution by more than five folds.

In a very recent theoretical paper, Cobos and Khair [27] developed a spectral element algorithm to compute the electrophoretic velocity of a spherical dielectric particle with arbitrary EDL thickness over a wide range of DC electric fields. They reported that the nonlinear contribution to the electrophoretic velocity of moderately charged particles ($\sigma a/\varepsilon\phi \sim 1$) grows as the electric field increases, whose onset is a function of the dimensionless particle radius, κa. It, however, vanishes at high electric fields ($Ea/\phi \gg 1$) with the electrophoretic velocity approaching the Hückel limit [27]. The authors further reported that their computed values for the electrophoretic velocity of highly charged particles ($\sigma a/\varepsilon\phi \gg 1$) under the thin EDL limit ($\kappa a \gg 1$) match the asymptotic result from Schnitzer and Yariv [10] and as well the experimental result from Tottori et al. [15].

Our previous work [21] presented a systematic experimental study of the effects of buffer concentration, particle size and surface charge on the electrophoretic velocity of spherical polystyrene particles in a straight rectangular microchannel. We demonstrated that the measured nonlinear electrophoretic particle velocity exhibits a 2(±0.5)-order dependence on the applied electric field of up to 3 kV/cm, within the theoretically predicted 3- and 3/2-order dependences [7-10]. We also found that the nonlinear electrophoretic mobility and index both decrease with increasing buffer concentration and particle size but increase with increasing particle charge, consistent with the theoretical predictions for high electric fields ($Ea/\phi \gg 1$).

As discussed above and in the review article from Khair [22], existing theories [3-10,27] and experiments [11-21,23-26] in nonlinear electrophoresis have all been concerned with spherical particles only. It is important to understand the effect of particle shape on this phenomenon, if any, because many relevant particles in electrophoresis, such as DNA molecules [28], viruses [29], bacteria [30], synthesized fibers [31] and hematite particles [32], possess non-spherical shapes. There have been several studies on the linear electrophoresis of non-spherical particles using weak-field models [33-38]. The electrophoretic velocity is given by Smoluchowski's formula under the thin EDL limit ($\kappa a \gg 1$) regardless of the particle shape [39]. It, however, departs from that formula and becomes dependent on the particle shape for moderately charged particles ($\sigma a/\varepsilon\phi \sim 1$) even with very thin EDLs because of the surface conduction effect [40-42]. This experimental work is aimed to investigate the effect of particle shape on electrophoresis in a wide range of electric fields ($Ea/\phi \gg 1$). We will test two types of non-spherical particles in a rectangular microchannel and compare their nonlinear electrophoretic behaviors against those of spherical particle with a similar diameter and surface charge. We will also study the nonlinear electrophoretic velocity of non-spherical particles in buffers of varying concentrations and compare the results with those obtained for spherical particles in our previous work [21].

2 Materials and methods

2.1 Microchannel and chemicals

A straight rectangular microchannel was used in the experiment. It was fabricated from polydimethylsiloxane (PDMS) via the standard soft-lithography technique [43]. The channel is 1 cm long with a uniform width and depth of approximately 50 μm each. Our experiment studied the nonlinear electrophoretic motion of various shaped rigid polystyrene particles, including 5.0 μm-diameter spherical particle (Sigma-Aldrich), 3.5 μm-diameter/6.0 μm-length peanut-shaped particle (Magsphere Inc.), and 3.8 μm-diameter/5.1 μm-length pear-shaped particle (Magsphere Inc.). The equivalent spherical diameters of the two non-spherical particles, which were obtained from their calculated total volumes in COMSOL®, are approximately identical and are only about 15% smaller than that of the spherical particle (Table 1). These particles were each resuspended in 0.025 mM phosphate buffer solution for an investigation of the particle shape effect on nonlinear electrophoresis. The particle concentration was kept low in each suspension (around 10^5 particles per ml) to minimize the particle-particle interactions. The Debye length in this solution was estimated to be about $1/\kappa = 63$ nm, such that the dimensionless particle radius is $\kappa a = 40 \gg 1$ for the 5.0 μm-diameter spherical particle, satisfying the thin EDL condition. It is noted that the threshold value of κa for this assumption may vary among different studies [e.g., 40]. To quantify the analysis, we define a dimensionless particle slenderness, ϵ,

$$\epsilon = \frac{a}{b} \tag{1}$$

where a is the maximum radius of the particle perpendicular to its long axis (or the half-length of the particle's short-axis), and b is the half-length of the particle along its long axis (or the half-length of the particle's long-axis). We also studied the effect of buffer concentration on the nonlinear electrophoresis of peanut-shaped particles. Table 1 summarizes the dimensions and slenderness values of the three types of particles used in the experiment.

Particle shape	$2a$ (μm)	$2b$ (μm)	Eq. diameter (μm)	Slenderness $\epsilon = a/b$
Sphere	5.0	5.0	5.0	1.0
Pear	3.8	5.1	4.3	0.75
Peanut	3.5	6.0	4.2	0.58

2.2 Experimental techniques

The electrokinetic motion of particles through the microchannel was driven by a high-voltage DC power supply (Glassman High Voltage). The electric field was varied from 0.1 to 5 kV/cm in each test, corresponding to $1 \leq \beta \leq 50$ for 5.0 μm diameter particles. The run of each test was kept no more than 15 s for each direction of electric field to minimize the influences of both Joule heating and backflow as detailed in our previous work [21]. Briefly, the effect of Joule heating was estimated to be insignificant because the temporal variation of electric current was observed to be no more than 10% even in the highest-concentration buffer under the highest electric field [44]. Moreover, the liquid levels in the end-channel reservoirs were balanced prior to every test to avoid the pressure-driven particle motion. The spherical and non-spherical particles were observed to move in the direction of the imposed DC electric field in all cases tested. This phenomenon indicates that the electroosmotic fluid flow is stronger than the electrophoretic particle motion, the latter of which is against the direction of electric field because of the naturally negative charge of particles [45,46]. The particle motion was visualized using an inverted microscope imaging system (Nikon Eclipse TE2000U, Nikon Instruments) and recorded through a CCD camera (Nikon DS-Qi1Mc) in a binning mode. The captured images were processed using the Nikon imaging software (NIS-Elements AR 2.30). The particle velocity was measured using the particle tracking velocimetry, where (at least) five particles travelling along the centerline of the microchannel were tracked to obtain an average for each electric field.

2.3 Experimental data analysis

We used the approach detailed in our previous work [21] to process the experimentally measured data of particle velocity, $V_p = V_{eo} + V_{ep}$, which is a result of the summation of the electroosmotic fluid velocity, V_{eo}, and electrophoretic particle velocity, V_{ep}. Briefly, we break down V_{ep} into the linear component, $V_{ep}^{(1)}$, and nonlinear component, $V_{ep}^{(n)}$, leading to

$$V_p = V_{ek} + V_{ep}^{(n)} = \mu_{ek}E + \mu_{ep}^{(n)}E^n \qquad (2)$$

where $V_{ek} = V_{eo} + V_{ep}^{(1)} = \mu_{ek}E$ is the traditionally defined (linear) electrokinetic particle velocity with μ_{ek} being the (linear) electrokinetic mobility, and $\mu_{ep}^{(n)}$ is the nonlinear electrophoretic mobility with the nonlinear index of electric field $n > 1$. Under the assumption that $V_{ep}^{(n)} \ll V_{ek}$ and hence $V_p \cong V_{ek}$ at small electric fields [15], we determined μ_{ek} through a linear regression of V_p for $E \leq 500$ V/cm. The nonlinear electrophoretic velocity, $V_{ep}^{(n)}$, was then obtained by subtracting $\mu_{ek}E$ from the measured V_p values at higher electric fields. The intercept and slope of the plot of $V_{ep}^{(n)}$ vs. E in the log-log space give the nonlinear electrophoretic mobility, $\mu_{ep}^{(n)}$, and nonlinear index, n, respectively.

3 Results and discussion

3.1 Orientation of non-spherical particles in electrophoresis

Figure 1A shows an image of the peanut- and pear-shaped particles, which were mixed with the spherical particles in 0.025 mM buffer for easy visualization, under the application of 0.2 kV/cm DC electric field. Both types of non-spherical particles were observed to quickly align their long-axes with the electric field direction and travel along with the spherical particle (nearly) at the center plane of the microchannel. These observations are consistent with the phenomena reported in previous studies, which arise from the combined action of the Maxwell and hydrodynamic stresses in the presence of the insulating channel walls [47-49]. We also noticed that the pear-shaped particles may travel with their heads or tails (highlighted in Fig. 1A) leading, the percentage of which is approximately 50% each. We measured the velocity of pear-shaped particles, V_p, at either orientation for electric field ranging from 0.1 to 0.4 kV/cm (note the identification of particle orientation gets more difficult at higher electric fields). As viewed from Fig. 1B, V_p scales linearly with the electric field strength as nonlinear electrophoresis is negligible at small electric fields such that $V_p \cong V_{ek} = \mu_{ek} E$. Moreover, it exhibits an insignificant dependence (less than 5% difference between the slopes of the two linear trendlines, i.e., μ_{ek}) on the particle orientation at every electric field. Therefore, we did not attempt to identify the orientation of pear-shaped particles at higher electric fields for a convenient study of nonlinear electrophoresis. We admit this treatment may cause certain errors, for example, the influence of particle orientation on nonlinear electrophoresis may no longer be negligible at high electric fields.

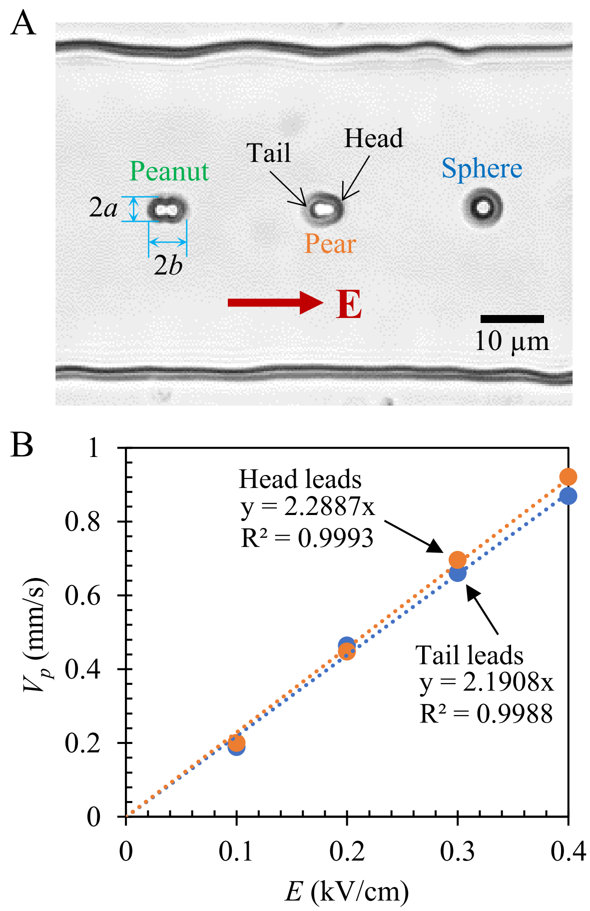

Figure 1. Electrophoresis of non-spherical particles in 0.025 mM buffer in a rectangular microchannel under electric field ranging from 0.1 to 0.4 kV/cm: (A) Microscopic images of the peanut- and pear-shaped particles along with a spherical particle, whose long-axes are aligned with the imposed DC electric field of 0.2 kV/cm. The lengths of the short- and long-axes of a non-spherical particle are highlighted; (B) Plot of the measured particle velocity (symbols), V_p, for the pear-shaped particles with heads and tails (highlighted on the image in A) leading the motion, respectively. The dotted lines are the linear trendlines to the experimental data for these two orientation cases with the corresponding equations and R-squared values being both displayed.

3.2 Effect of particle shape on nonlinear electrophoresis

Figure 2A shows the experimentally measured V_p for the three types of particles in 0.025 mM buffer under electric field ranging from 0.1 to 5 kV/cm. There is an insignificant gap among the three linear trendlines (i.e., V_{ek}) to the data points for 0.5 kV/cm and below, indicating approximately identical values of electrokinetic mobility (with 5% variation), $\mu_{ek} = 2.23(\pm 0.11) \times 10^{-8}$ m^2/V·s, for the spherical and non-spherical particles. Therefore, the particle zeta potential can be viewed to remain similar among these particles under the thin EDL limit [39], so that any different nonlinear behaviors witnessed in Fig. 2A can be viewed more closely associated with the particle shape. For electric fields above 1 kV/cm, the data of V_p start increasingly deviating from the linear trendline for each type of particles in Fig. 2A. Moreover, this deviation exhibits a visible dependence on the particle shape, which is evidenced from the dissimilar power trendlines to the data of nonlinear electrophoretic velocity, $V_{ep}^{(n)} = V_p - V_{ek}$, in Fig. 2B. The peanut-shaped particles appear to have the largest $V_{ep}^{(n)}$. The spherical and pear-shaped particles display weaker while overall similar nonlinear behaviors in $V_{ep}^{(n)}$ over the range of electric fields under test.

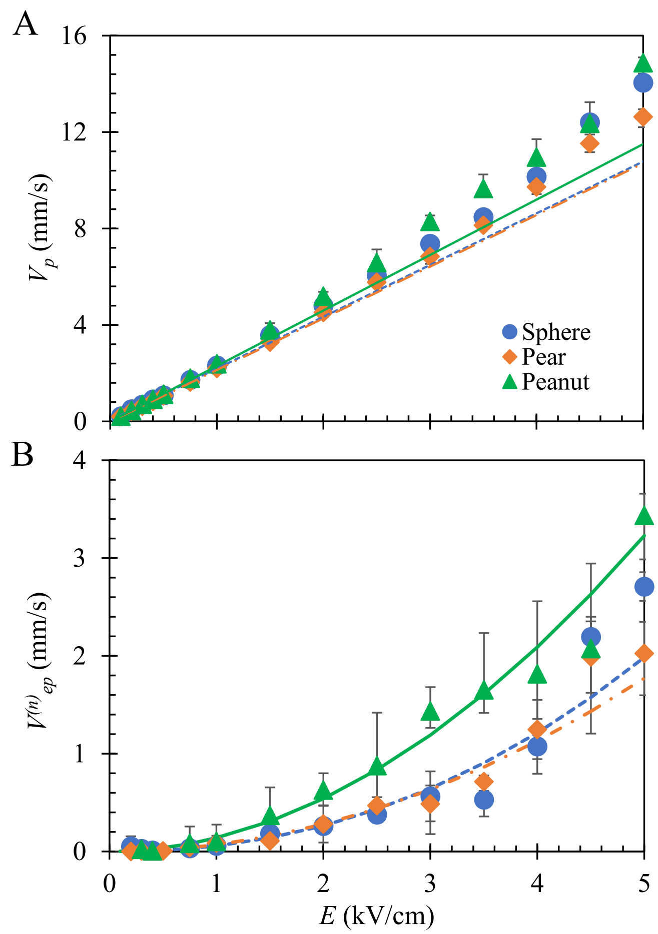

Figure 2. Electrophoresis of spherical, pear and peanut-shaped particles in 0.025 mM buffer under electric field ranging from 0.1 to 5 kV/cm: (A) Experimentally measured velocity (symbols with error bars; note some of the error bars are within the symbol size and become invisible), V_p, where the linear trendlines are the best fits for the experimental data points at 0.5 kV/cm and below (assumed to represent the linear electrokinetic particle velocity, V_{ek}); (B) Experimentally obtained (symbols with error bars) nonlinear electrophoretic velocity, $V_{ep}^{(n)} = V_p - V_{ek}$, vs. electric field, where the curves are the positive power trendlines best fitted for the experimental data points.

To further compare the nonlinear electrophoretic behaviors of spherical and non-spherical particles, we replot the data of $V_{ep}^{(n)}$ vs. electric field in the log-log space. As seen from Fig. 3A, the power trendline in Fig. 2B for each type of particles now turns into a linear trendline, whose y-intercept and slope yield the nonlinear electrophoretic mobility, $\mu_{ep}^{(n)}$, and nonlinear index of electric field, n, respectively. Interestingly, the three linear trendlines in Fig. 3A are roughly parallel indicating marginal differences in n among the three types of particles. However, the peanut-shaped particle has an apparently greater $\mu_{ep}^{(n)}$ than the spherical and pear-shaped ones. Fig. 3B compares the obtained values of $\mu_{ep}^{(n)}$ and n among the three types of particles in terms of the particle slenderness, $\epsilon = a/b$, in Eq. (1). One can see a decrease of $\mu_{ep}^{(n)}$ while an increase of n with the increase of ϵ from the peanut to pear and spherical particles. However, the value of n still stays at around 2, which is consistent with our recent experiment [21] and within the range of theoretical predictions [7-10] for spherical particles at high electric fields. Referring to the findings in our previous study that $\mu_{ep}^{(n)}$ and n both become greater for smaller spherical particles [21], we speculate that the decreasing trend of $\mu_{ep}^{(n)}$ with the increase of ϵ may be a result of the increasing particle radius, a, perpendicular to the particle moving direction (i.e., the direction of the imposed DC electric field, see Fig. 1A and Table 1), which plays an important role in the drag force [50]. In contrast, the increasing trend of n with the increase of ϵ may arise from the decreasing particle length along the electric field direction, leading to a larger curvature of the particle surface and hence a stronger surface conduction effect within the EDL [22,27].

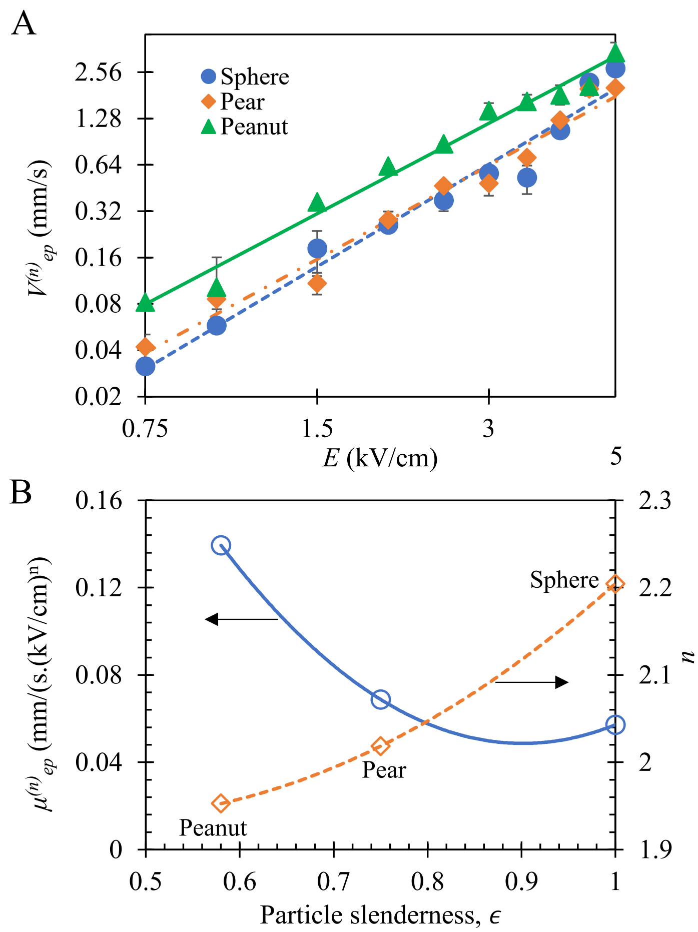
A
Sphere
Pear
Peanut
2.56
1.28
0.64
0.32
0.16
0.08
0.04
0.02
$V^{(n)}_{ep}$ (mm/s)
0.75
1.5
3
5
E (kV/cm)
B
0.16
0.12
0.08
0.04
0
2.3
2.2
2.1
2
1.9
$\mu^{(n)}_{ep}$ (mm/(s.(kV/cm)^n))
n
Sphere
Pear
Peanut
0.5
0.6
0.7
0.8
0.9
1
Particle slenderness, ϵ

1

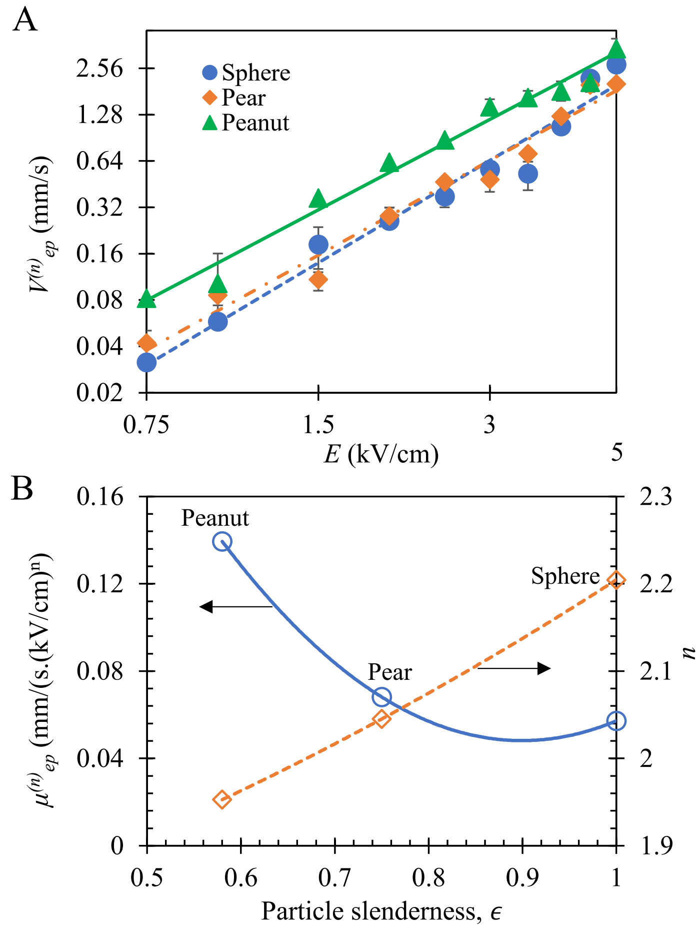

Figure 3. Nonlinear electrophoresis of spherical, pear and peanut-shaped particles in 0.025 mM buffer: (A) Experimentally obtained (symbols with error bars) nonlinear electrophoretic velocity, $V_{ep}^{(n)}$, vs. electric field in the log-log space, where the linear trendlines are the best fits to the data points; (B) Comparison of the nonlinear electrophoretic mobility, $\mu_{EP}^{(n)}$, and nonlinear index of electric field, n, as a function of the particle slenderness. The lines are used to guide the eyes only.

3.3 Effect of buffer concentration on nonlinear electrophoresis of non-spherical particles

Our previous work demonstrates that spherical particles exhibit stronger nonlinear electrophoresis in lower-concentration buffer solutions [21] because of the thicker EDL and hence stronger surface conduction effects therein [7-10]. This trend should remain valid for non-spherical particles as the impact of buffer concentration on the ionic fluxes within and across the EDL is intuitively independent of particle shape. Fig. 4A displays the experimentally obtained data of $V_{ep}^{(n)}$ vs. electric field for the peanut-shaped particles in 0.01, 0.025 and 0.05 mM buffers along with the corresponding power trendlines. Like the spherical particles in our previous study [21], non-spherical particles overall also have larger values of $V_{ep}^{(n)}$ in the lower-concentration buffers at each imposed electric field. Moreover, the differences in $V_{ep}^{(n)}$ among the three buffer concentrations get increasingly large under higher electric fields. Fig. 4B shows the extracted nonlinear electrophoretic components $\mu_{EP}^{(n)}$ and n as a function of the buffer concentration. As expected, both $\mu_{ep}^{(n)}$ and n exhibit a decreasing trend with the increase of buffer concentration for the peanut-shaped particles. Moreover, the values of n are still within the range of 3/2 and 2, consistent with the theoretical prediction of nonlinear electrophoresis for spherical particles at high electric fields [7-10]. Similar results are also obtained for the pear-shaped particles in buffers of varying concentrations (see the Supporting Information).

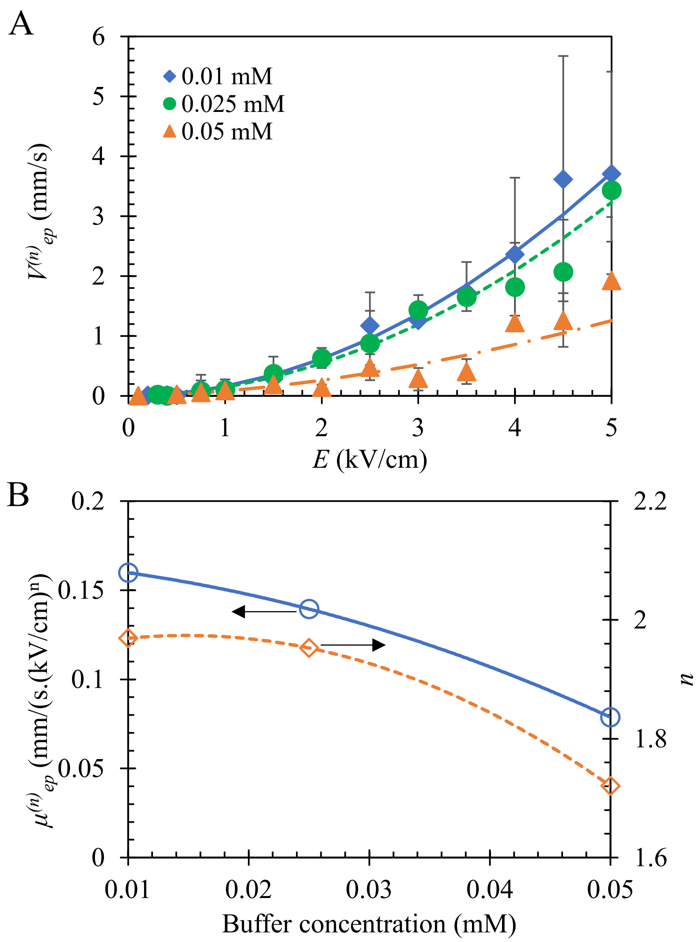

Figure 4. Nonlinear electrophoresis of peanut-shaped particles in buffer solutions with varying concentrations: (A) Experimentally obtained (symbols with error bars) nonlinear electrophoretic velocity, $V_{ep}^{(n)}$, vs. electric field, where the curves are the positive power trendlines best fitted for the data points; (B) Comparison of the nonlinear electrophoretic mobility, $\mu_{EP}^{(n)}$, and nonlinear index of electric field, n, with respect to the buffer concentration. The lines are used to guide the eyes only.

4 Concluding remarks

We have built upon our previous work [21] to experimentally study the effect of particle shape on nonlinear electrophoresis of rigid particles in a rectangular microchannel under high electric fields.

Both peanut- and pear-shaped particles have been tested along with spherical particles with approximately similar diameter and surface charge. A dimensionless parameter, i.e., particle slenderness ϵ, is defined to quantify the particle shape, which increases from for the peanut- to pear-shaped and spherical particles. We find that the nonlinear electrophoretic mobility $\mu_{ep}^{(n)}$ decreases with the increasing particle slenderness while the opposite goes to the nonlinear index n of electric field. It is speculated that these two trends may be associated with the particle dimension along and perpendicular to the electric field direction, respectively. We also find that the nonlinear index n for each type of non-spherical particles is still within the theoretically predicted range for spherical particles at high electric fields. Moreover, both $\mu_{ep}^{(n)}$ and n are found to increase in a lower-concentration buffer solution regardless of the particle shape. It is important to note that our experiments in both this and the earlier work [21] have been restricted to dilute particle suspensions. We will study in future work if and how the particle-particle interaction may affect the nonlinear electrophoretic behavior at high electric fields.

This work was supported in part by NSF under grant number CBET-2100772 and CBET-2127825.

The authors have declared no conflict of interest.

Data availability statement

The data that support the findings of this study are available from the corresponding author upon reasonable request.

5 References

[1] Lyklemma J. Fundamentals of Interface and Colloid Science. Cambridge, MA: Academic Press; 1991.

[2] Chang HC, Yeo LY. Electrokinetically Driven Microfluidics and Nanofluidics. New York: Cambridge University Press; 2010.

[3] Dukhin SS, Shilov VN. Kinetic aspects of electrochemistry of disperse systems. Part II. Induced dipole moment and the non-equilibrium double layer of a colloid particle. Adv Colloid Interface Sci. 1980;13:153–95.

[4] Dukhin SS. Electrophoresis at large Peclet numbers. Adv Colloid Interface Sci. 1991;6:219-48.

[5] Mishchuk NA. Concentration polarization of interface and non-linear electrokinetic phenomena. Adv Colloid Interface Sci. 2010;160:16-39.

[6] Schnitzer O, Yariv E. Macroscale description of electrokinetic flows at large zeta potentials: nonlinear surface conduction. Phys Rev E. 2012;86;021503.

[7] Mishchuk NA, Dukhin SS. Electrophoresis of solid particles at large Peclet numbers. Electrophoresis. 2002;23:2012–22.

[8] Shilov V, Barany S, Grosse C, Shramko O. Field-induced disturbance of the double layer electro-neutrality and non-linear electrophoresis. Adv Colloid Interface Sci. 2003;104:159–73.

[9] Schnitzer O, Zeyde R, Yavneh I, Yariv E. Weakly nonlinear electrophoresis of a highly charged colloidal particle. Phys Fluids. 2013;25:052004.

[10] Schnitzer O, Yariv E. Nonlinear electrophoresis at arbitrary field strengths: small-Dukhin-number analysis. Phys Fluids. 2014;26:122002.

[11] Kontush SM, Dukhin SS, Vidov OI. Aperiodic electrophoresis. Kolloidnyi Zh. (in Russian). 1994;56:654–60.

[12] Barany S. Electrophoresis in strong electric fields. Adv Colloid Interface Sci. 2009;147–148: 36–43.

[13] Mishchuk NA, Barinova NO. Theoretical and Experimental Study of Nonlinear Electrophoresis. Colloid J. 2011;73:88–96.

[14] Youssefi MR, Diez FJ. Ultrafast electrokinetics. Electrophoresis. 2016;37:692-8.

[15] Tottori S, Misiunas K, Keyser UF. Nonlinear electrophoresis of highly charged nonpolarizable particles. Phys Rev Lett. 2019;123:014502.

[16] Cardenas-Benitez B, Jind B, Gallo-Villanueva RC, Martinez-Chapa SO, Lapizco-Encinas BH, Pérez-González VH. Direct current electrokinetic particle trapping in insulator-based microfluidics: Theory and experiments. Anal Chem. 2020;92:12871−9.

[17] Coll De Peña A, Miller A, Lentz CJ, Hill N, Parthasarathy A, Hudson AO, Lapizco-Encinas BH. Creation of an electrokinetic characterization library for the detection and identification of biological cells. Anal Bioanal Chem. 2020;412:3935–45.

[18] Antunez-Vela S, Perez-Gonzalez VH, De Peña AC, Lentz CJ, Lapizco-Encinas BH. Simultaneous determination of linear and nonlinear electrophoretic mobilities of cells and microparticles. Anal Chem. 2020;92:14885–91.

[19] Ruz-Cuen R, de los Santos-Ramírez JM, Cardenas-Benitez B, Ramírez-Murillo CJ, Miller A, Hakim K, Lapizco-Encinas BH, Perez-Gonzalez VH. Amplification factor in DC insulator-based electrokinetic devices: a theoretical, numerical, and experimental approach to operation voltage reduction for particle trapping. Lab Chip. 2021;21:4596-607.

[20] Vaghef-Koodehi A, Dillis C, Lapizco-Encinas BH. High-resolution charge-based electrokinetic separation of almost identical microparticles. Anal Chem. 2022;94:6451-6.

[21] Bentor J, Dort H, Chitrao R, Zhang Y, Xuan X., Nonlinear electrophoresis of dielectric particles in Newtonian fluids. Electrophoresis 2023;44:938-46.

[22] Khair AS. Nonlinear electrophoresis of colloidal particles. Current Opinion Colloid Interface Sci. 2022;59:101587.

[23] Ernst OD, Vaghef-Koodehi A, Dillis C, Lomeli-Martin A, Lapizco-Encinas BH. Dependence of nonlinear electrophoresis on particle size and charge. Anal Chem 2023;95: 6595–602.

[24] Lomeli-Martin A, Ernst OD, Cardenas-Benitez B, Cobos R, Khair AS, Lapizco-Encinas BH. Characterization of the nonlinear electrophoretic behavior of colloidal particles in a microfluidic channel. Anal Chem 2023;95:6740−7.

[25] Vaghef-Koodehi A, Ernst OD, Lapizco-Encinas BH. Separation of cells and microparticles in insulator-based electrokinetic systems. Anal Chem 2023;95:1409−18.

[26] Ahamed NNN, Mendiola-Escobedo CA, Ernst OD, Perez-Gonzalez VH, Lapizco-Encinas BH. Fine-tuning the characteristic of the applied potential to improve AC-iEK separations of microparticles. Anal Chem 2023;95:9914−23.

[27] Cobos R, Khair AS. Nonlinear electrophoretic velocity of a spherical colloidal particle. J Fluid Mech 2023;968:A14.

[28] Allison S, Chen C, Stigter D. The length dependence of translational diffusion, free solution electrophoretic mobility, and electrophoretic tether force of rigid rod-like model duplex DNA. Biophys J 2001;81:2558–68.

[29] Kang K, Dhont JKG. Electric-field induced transitions in suspensions of charged colloidal rods. Soft Matt 2010;6:273–86.

[30] Hakim KS, Lapizco-Encinas BH. Analysis of microorganisms with nonlinear electrokinetic microsystems. Electrophoresis 2021;42:588-604.

[31] Chen SB, Koch DL. Electrophoresis and sedimentation of charged fibres. J Colloid Interface Sci 1996;180:466–77.

[32] Rica RA, Jimenez ML, Delgado AV. Electrokinetics of concentrated suspensions of spheroidal hematite nanoparticles. Soft Matt 2012;8:3596–607.

[33] Sherwood JD. Electrophoresis of rods. J Chem Soc Faraday Trans 2 1982;78:1091–100.

[34] O'Brien R, Ward D. The electrophoresis of a spheroid with a thin double layer. J Colloid Interface Sci 1988;121:402–13.

[35] Keh HJ, Huang TY. Diffusiophoresis and electrophoresis of colloidal spheroids. J Colloid Interface Sci 1993;160:354–71.

[36] Bach GA, Hollingsworth AD, Koch DL. Electrophoretic mobility of rigid rodlike particles in dilute aqueous and glycerol suspensions: comparison between theory and experiment. J Colloid Interface Sci 2002;251:208–13.

[37] Yariv E. Slender-body approximations for electro-phoresis and electro-rotation of polarizable particles. J Fluid Mech 2008;613:85–94.

[38] Yariv E, Schnitzer O. The electrophoretic mobility of rod-like particles. J Fluid Mech 2013;719:R3.

[39] Morrison FA. Electrophoresis of a particle of arbitrary shape. J Colloid Interface Sci 1970;34:210-4.

[40] O'Brien RW, White LR. Electrophoretic mobility of a spherical colloidal particle. J Chem Soc Faraday Trans 1978;74:1607-26.

[41] O'Brien RW. The solution of the electrokinetic equations for colloidal particles with thin double layers. J Colloid Interface Sci 1983;92:204-16.

[42] Keh HJ, Chen SB. Diffusiophoresis and electrophoresis of colloidal cylinders. Langmuir 1993;9:1142–9.

[43] Zhu J, Xuan X. Dielectrophoretic focusing of particles in a microchannel constriction using DC-biased AC electric fields. Electrophoresis. 2009;30:2668-75.

[44] Xuan X. Review of nonlinear electrokinetic flows in insulator-based dielectrophoresis: From induced charge to Joule heating effects. Electrophoresis. 2022;43:167–89.

[45] Hunter RJ. Zeta Potential in Colloid Science. New York: Academic Press; 1981.

[46] Kirby BJ, Hasselbrink Jr EF. Zeta potential of microfluidic substrates: 2. Data for polymers. Electrophoresis. 2004;25:203-13.

[47] Ai Y, Beskok A, Gauthier DT, Joo SW, Qian S. dc electrokinetic transport of cylindrical cells in straight microchannels. Biomicrofluid 2009;3:044110.

[48] Liang L, Ai Y, Zhu J, Qian S, Xuan X. Wall-induced lateral migration in particle electrophoresis through a rectangular microchannel. J Colloid Interface Sci 2010;347:142-6.

[49] Xuan X. Recent advances in direct current electrokinetic manipulation of particles for microfluidic applications. Electrophoresis. 2019;40:2484-513.

[50] Happel J, Brenner H. Low Reynolds Number Hydrodynamics. Prentice-Hall; 1965.